

Polarization structure of the radiation scattered from an optically active disperse medium

G.M. Krekov,¹ M.M. Krekova,¹ and V.N. Kuz'min²

¹ *Institute of Atmospheric Optics,
Siberian Branch of the Russian Academy of Sciences, Tomsk, Russia*

² *Institute of Physics,
Belarus Academy of Sciences, Minsk, Belarus*

Received October 2, 2003

The possibility of developing Monte Carlo statistical algorithms for solving the radiative transfer equation in the vector form is demonstrated. The efficiency of such an algorithm is tested, and the polarization structure of a return signal is analyzed tentatively using a model medium consisting of gyrotropic scattering particles.

Introduction

In applications of physical optics, in particular, to optics of the atmosphere and hydrosphere, it is often necessary to take into account the anisotropy of scattering particles. Such particles may present, for example, in the tropospheric aerosol of the soil-erosion origin (whose main component is quartz), in a hydrosol as some types of organic particles, and in clouds as ice crystals. Weak manifestations of the optical activity of natural disperse media under natural conditions may intensify under extreme perturbations of the electric field (the square-law Kerr effect). Thus, for example, in Ref. 1 it was shown that in the period prior to seismic events the electric field strength redistributes spatially over local volumes of the earth's crust. In Ref. 2 it was shown that these variations of δE markedly manifest themselves through the anisotropy factor, and polarimetric indices of the earth's crust transform in such cases. It is quite probable that their effect on the aerosol particles of soil-erosion origin will be similar.

Optical properties of the elementary scattering volume of an anisotropic medium not always can be described by the characteristics of an equivalent isotropic medium.³ Estimations of the energy characteristic of radiation are usually restricted to consideration of the scalar transfer equation. For optically active media, this approach is not justified physically, and it may prove necessary already for estimation of the radiation intensity to solve the system of integro-differential equations for the Stokes vector-parameters.⁴ Polarization effects are taken into account in analyzing the radiation propagation through anisotropic media in a number of astrophysical problems.⁵ The asymptotic method for calculation of the Stokes vector-function in the case of illumination of the medium consisting of randomly oriented anisotropic particles by an infinitely wide light beam was developed in Ref. 6. The method of statistical simulation is optimal for studying the radiation

propagation in a medium, where deep conditions fail. This paper proposes an approach to construction of the statistical simulation algorithm for estimating the linear functionals of the solution of the radiative transfer equation in a vector form.

Method of solution

In the general case, the radiative transfer equation with regard for polarization has the form

$$\boldsymbol{\omega}\nabla\mathbf{I}(\mathbf{r}, \boldsymbol{\omega}) = -\boldsymbol{\sigma}(\mathbf{r})\mathbf{A}(\mathbf{r})\mathbf{I}(\mathbf{r}, \boldsymbol{\omega}) + \boldsymbol{\sigma}(\mathbf{r})\mathbf{B}(\mathbf{r}, \boldsymbol{\omega}); \quad (1)$$

$$\mathbf{B}(\mathbf{r}, \boldsymbol{\omega}) = \frac{\Lambda(r)}{4\pi} \int \mathbf{P}(\mathbf{r}, \boldsymbol{\omega}, \boldsymbol{\omega}')\mathbf{I}(\mathbf{r}, \boldsymbol{\omega}') d\boldsymbol{\omega}'; \quad (2)$$

$$\mathbf{P}(\mathbf{r}, \boldsymbol{\omega}, \boldsymbol{\omega}') = \mathbf{L}(\pi - i_2)\mathbf{R}(\mathbf{r}, \boldsymbol{\omega}, \boldsymbol{\omega}')\mathbf{L}(-i_1), \quad (3)$$

where $\mathbf{I} = (I, Q, U, V)$ is the Stokes vector parameter; $\boldsymbol{\omega} = (a, b, c)$ is the unit vector of the direction $\mathbf{r} = (x, y, z)$; $\boldsymbol{\sigma}$ is the extinction coefficient; Λ is the single scattering albedo; \mathbf{A} is the extinction matrix normalized to $\boldsymbol{\sigma}$; \mathbf{P} is the angular matrix; \mathbf{R} is the scattering phase matrix; \mathbf{L} is the rotation matrix⁷; i_1 and i_2 are the angles between the scattering plane and planes including the axis of the coordinate system and the vectors $\boldsymbol{\omega}$ and $\boldsymbol{\omega}'$, respectively.

The algorithms of the Monte Carlo method, in particular, for solution of the radiative transfer equation are most correctly constructed based on the integral equation in the probabilistic interpretation of its kernel. For an isotropic medium, the transition from a system of integro-differential equations to a system of integral equations is shown, e.g., in Ref. 8.

For some anisotropic media, this transition can be performed using the method of normal waves,⁴ where the extinction matrix \mathbf{A} is diagonalized using some numerical matrix \mathbf{T} . By multiplying Eq. (1) by \mathbf{T} we obtain

$$\boldsymbol{\omega}\nabla\mathbf{T}\mathbf{I}(\mathbf{r}, \boldsymbol{\omega}) = -\boldsymbol{\sigma}(\mathbf{r})\mathbf{T}\mathbf{A}(\mathbf{r})\mathbf{T}^{-1}\mathbf{T}\mathbf{I}(\mathbf{r}, \boldsymbol{\omega}) + \boldsymbol{\sigma}(\mathbf{r})\mathbf{T}\mathbf{B}(\mathbf{r}, \boldsymbol{\omega}). \quad (4)$$

Here the matrix \mathbf{TAT}^{-1} has a diagonal form, which allows Eq. (4) to be solved for \mathbf{TI} , if \mathbf{TB} is assumed a known vector function. Multiplication by \mathbf{T}^{-1} gives a system of integral equations for \mathbf{I} , whose structure is determined by the matrix \mathbf{A} .

Let us consider, as an example the medium consisting of randomly oriented particles having no symmetry planes and, consequently, neither symmetry axes nor symmetry centers (isotropic gyrotropic medium). The extinction and scattering phase matrices in this case have the forms⁹:

$$\mathbf{A} = \begin{pmatrix} 1 & 0 & 0 & \gamma_{14} \\ 0 & 1 & \gamma_{23} & 0 \\ 0 & -\gamma_{23} & 1 & 0 \\ \gamma_{14} & 0 & 0 & 0 \end{pmatrix};$$

$$\mathbf{R} = \begin{pmatrix} R_{11} & R_{12} & R_{13} & R_{14} \\ R_{12} & R_{22} & R_{23} & R_{24} \\ -R_{13} & -R_{23} & R_{33} & R_{34} \\ R_{14} & R_{24} & -R_{34} & R_{44} \end{pmatrix},$$

$\mathbf{R}(\mathbf{r}, \boldsymbol{\omega}, \boldsymbol{\omega}') = \mathbf{R}(\mathbf{r}, \boldsymbol{\omega}\boldsymbol{\omega}')$. For the given matrix \mathbf{A} , the matrices \mathbf{T} and \mathbf{T}^{-1} are determined as follows

$$\mathbf{T} = \begin{pmatrix} 1 & 0 & 0 & 0 \\ 0 & 1 & i & 0 \\ 0 & 1 & -i & 0 \\ 1 & 0 & 0 & -1 \end{pmatrix}, \quad \mathbf{T}^{-1} = \frac{1}{\sqrt{2}} \begin{pmatrix} 1 & 0 & 0 & 0 \\ 0 & 1 & 1 & 0 \\ 0 & -i & i & 0 \\ 1 & 0 & 0 & 1 \end{pmatrix} \quad (6)$$

and, consequently,

$$\mathbf{TAT}^{-1} = \begin{pmatrix} 2(1 + \chi_{14}) & 0 & 0 & 0 \\ 0 & 2(1 - i\chi_{23}) & 0 & 0 \\ 0 & 0 & 2(1 + i\chi_{23}) & 0 \\ 0 & 0 & 0 & 2(1 - \chi_{14}) \end{pmatrix}. \quad (7)$$

The boundary conditions are believed preset in the plane $Y=0$, and assuming the vector function $\mathbf{I}_0(\mathbf{r}_0, \boldsymbol{\omega})$ known at $b > 0$:

$$\boldsymbol{\alpha}(\mathbf{r}, \mathbf{r}_0) = e^{-\tau(\mathbf{r}, \mathbf{r}_0)} \begin{pmatrix} e^{-v_{14}(\mathbf{r}, \mathbf{r}_0)} & 0 & 0 & 0 \\ 0 & e^{iv_{23}(\mathbf{r}, \mathbf{r}_0)} & 0 & 0 \\ 0 & 0 & e^{-iv_{23}(\mathbf{r}, \mathbf{r}_0)} & 0 \\ 0 & 0 & 0 & e^{v_{14}(\mathbf{r}, \mathbf{r}_0)} \end{pmatrix},$$

where

$$\tau(\mathbf{r}, \mathbf{r}_0) = \frac{1}{by} \int_0^y \sigma(\mathbf{r}) d\xi; \quad v_{14} = \frac{1}{b} \int_0^y \sigma(\mathbf{r}') \gamma_{14}(\mathbf{r}') d\xi,$$

$$v_{23} = \frac{1}{b} \int_0^y \sigma(\mathbf{r}') \gamma_{23}(\mathbf{r}') d\xi; \quad \mathbf{r}' = \mathbf{r} + \frac{\xi - y}{b} \boldsymbol{\omega}.$$

The solution of the inhomogeneous equation for $\mathbf{TI}(\mathbf{r}, \boldsymbol{\omega})$ can be presented as

$$\mathbf{TI}(\mathbf{r}, \boldsymbol{\omega}) = \frac{1}{b} \int_0^y \sigma(\mathbf{r}') \boldsymbol{\alpha}(\mathbf{r}, \mathbf{r}') \mathbf{TB}(\mathbf{r}, \boldsymbol{\omega}) d\xi + \boldsymbol{\alpha}(\mathbf{r}, \mathbf{r}') \mathbf{TI}_0(\mathbf{r}, \boldsymbol{\omega}), \quad (9)$$

where the matrix $\boldsymbol{\alpha}(\mathbf{r}, \mathbf{r}')$ is obtained from the matrix $\boldsymbol{\alpha}(\mathbf{r}, \mathbf{r}_0)$ through the replacement of the lower integration limit 0 by ξ and \mathbf{r}' by $\mathbf{r}'' = \mathbf{r} + (\eta - y)\boldsymbol{\omega}/b$. Multiplying Eq. (9) by \mathbf{T}^{-1} gives the sought formal solution of Eq. (4) at $b > 0$:

$$\mathbf{I}(\mathbf{r}, \boldsymbol{\omega}) = \frac{1}{b} \int_0^y \sigma(\mathbf{r}') \mathbf{T}^{-1} \boldsymbol{\alpha}(\mathbf{r}, \mathbf{r}') \mathbf{TB}(\mathbf{r}', \boldsymbol{\omega}) d\xi + \mathbf{T}^{-1} \boldsymbol{\alpha}(\mathbf{r}, \mathbf{r}_0) \mathbf{TI}_0(\mathbf{r}, \boldsymbol{\omega}).$$

The matrix $\mathbf{F}(\mathbf{r}, \mathbf{r}') = \mathbf{T}^{-1} \boldsymbol{\alpha}(\mathbf{r}, \mathbf{r}') \mathbf{T}$ multiplied, for a convenience, by $e^{\tau(\mathbf{r}, \mathbf{r}')}$ can be reduced to the form

$$\mathbf{F}(\mathbf{r}, \mathbf{r}') = \begin{pmatrix} \cosh v_{14} & 0 & 0 & -\sinh v_{14} \\ 0 & \cos v_{23} & -\sin v_{23} & 0 \\ 0 & \sin v_{23} & \cos v_{23} & 0 \\ -\sinh v_{14} & 0 & 0 & \cosh v_{14} \end{pmatrix}. \quad (11)$$

By substituting Eqs. (2) and (11) into Eq. (10) we obtain the integral equation for the Stokes vector-function

$$\mathbf{I}(\mathbf{r}, \boldsymbol{\omega}) = \frac{1}{4\pi b} \int_0^y \sigma(\mathbf{r}) \lambda(\mathbf{r}) e^{-\tau(\mathbf{r}, \mathbf{r}')} \int_{4\pi} \mathbf{P}(\mathbf{r}', \boldsymbol{\omega}\boldsymbol{\omega}') \mathbf{I}(\mathbf{r}', \boldsymbol{\omega}') d\boldsymbol{\omega}' d\xi + e^{-\tau(\mathbf{r}, \mathbf{r}_0)} \mathbf{F}(\mathbf{r}, \mathbf{r}_0) \mathbf{I}_0(\mathbf{r}, \boldsymbol{\omega}), \quad b > 0.$$

After some simple transformations, Eq. (12) and that similar to it at $b < 0$ can be reduced to the following integral equation:

$$\mathbf{I}(\mathbf{X}) = \int_X \mathbf{K}_I(\mathbf{X}, \mathbf{X}') d\mathbf{X}' + \boldsymbol{\Psi}(\mathbf{X}) \quad (13)$$

with the kernel

$$\mathbf{K}_I(\mathbf{X}', \mathbf{X}) = \frac{\sigma(\mathbf{r}') \lambda(\mathbf{r}') e^{-\tau(\mathbf{r}, \mathbf{r}')} \mathbf{F}(\mathbf{r}, \mathbf{r}') \mathbf{P}(\mathbf{r}', \boldsymbol{\omega}, \boldsymbol{\omega}')}{4\pi |\mathbf{r} - \mathbf{r}'|^2} \delta\left(\boldsymbol{\omega} - \frac{\mathbf{r} - \mathbf{r}'}{|\mathbf{r} - \mathbf{r}'|}\right) \quad (14)$$

and the free term

$$\boldsymbol{\Psi}(\mathbf{X}) = e^{-\tau(\mathbf{r}, \mathbf{r}_0)} \mathbf{F}(\mathbf{r}, \mathbf{r}_0) \mathbf{I}_0(\boldsymbol{\omega}), \quad (15)$$

where \mathbf{X} is the phase space of coordinates and directions, $\mathbf{X} = (\mathbf{r}, \boldsymbol{\omega})$.

Equation (13) can be interpreted as the equation of transfer of the polarized light in a fixed isotropic medium with the extinction coefficient $\sigma(r)$ and the angular matrix of transformation of the Stokes parameters $\mathbf{F}(\mathbf{r}, \mathbf{r}') \mathbf{P}(\mathbf{r}, \boldsymbol{\omega}, \boldsymbol{\omega}')$. Then, for the collision density vector function $\boldsymbol{\varphi}(\mathbf{X}) = \sigma(\mathbf{r}) \mathbf{I}(\mathbf{X})$ we have

$$\boldsymbol{\varphi}(\mathbf{X}) = \int_X \mathbf{K}(\mathbf{X}', \mathbf{X}) \boldsymbol{\varphi}(\mathbf{X}') d\mathbf{X}' + \sigma(\mathbf{r}) \boldsymbol{\Psi}(\mathbf{X}); \quad (16)$$

$$\mathbf{K}(\mathbf{X}', \mathbf{X}) = \sigma(\mathbf{r})\mathbf{K}_I(\mathbf{X}', \mathbf{X}) / \sigma(\mathbf{r}). \quad (17)$$

This interpretation of Eq. (13) allows the Monte Carlo algorithms developed for the isotropic medium to be used with minor changes in the calculation of the linear functionals of $\boldsymbol{\varphi}$ [Ref. 6]. These changes largely deal with the procedure of recalculation of the Stokes vector-parameter after scattering, which, in contrast to that in Ref. 6, involves the following equations:

$$I = S_1 \cosh v_{14} - S_4 \sinh v_{14}; \quad Q = S_2 \cos v_{23} - S_3 \sin v_{23}; \\ U = S_2 \sin v_{23} + S_3 \cos v_{23}; \quad V = -S_1 \sinh v_{14} + S_4 \cosh v_{14},$$

where

$$S_1 = I'R_{11} + AR_{12} + BR_{13} + V'R_{14}, \\ S_2 = C \cos 2i_2 - D \sin 2i_2, \\ S_3 = C \sin 2i_2 + D \cos 2i_2, \\ S_4 = I'R_{41} + AR_{42} + BR_{43} + V'R_{44}; \quad (18) \\ A = Q' \cos 2i_1 - U' \sin 2i_1; \\ B = Q' \sin 2i_1 + U' \cos 2i_1; \\ C = I'R_{21} + AR_{22} + BR_{23} + V'R_{24}; \\ D = I'R_{31} + AR_{32} + BR_{33} + V'R_{34}.$$

However, it should be noted that Eq. (13) and, consequently, Eqs. (14), (15), and (18) are valid if the matrix \mathbf{A} is specified by Eq. (5). For other types of anisotropic media, where there are normal waves,² it is necessary to repeatedly derive (by the above scheme) the integral equation for the vector-function $\boldsymbol{\varphi}(\mathbf{X})$, since the diagonalizing matrix \mathbf{T} will have different form. Below we test the approach proposed using a particular example.

Calculated results

In Ref. 10 it was shown that the sensitivity of the optical characteristics to anisotropic properties of the medium manifests itself most strongly in the behavior of the components of the scattering phase matrix at the angles larger than 150° , that is, in the backward directions. Therefore, the initial and the boundary conditions of the problem correspond to the scheme of a monostatic lidar sensing. It is assumed that the linearly polarized light delta-pulse is incident on a plane-parallel homogeneous scattering layer Δy with the preset optical properties. A point source and a detector are located at the origin of coordinates, and their optical axes are normal to the layer. The source emits isotropically to the solid angle $2\pi(1 - \cos\varphi_{\text{source}})$, and the solid angle of the detector's field of view is $2\pi(1 - \cos\varphi_d)$. The lidar is spaced by y_0 from the medium. The whole set of the optical characteristics is precalculated taking into account anisotropy of spherical particles. The calculation was done for the wavelength of $0.5 \mu\text{m}$ and aerosol particles distributed according to the lognormal law with the median radius of $0.03 \mu\text{m}$ and the distribution variance of 0.74 [Ref. 11]. The refractive index is $n = (n_L + n_R)/2 = 1.55$, where n_L and n_R are the refractive indices for

the left and right circularly polarized waves, whose difference is proportional to the optical activity of the medium α_s , and in the calculations they were taken equal to 10^{-4} and 10^{-2} . Figure 1 shows the angular dependence of the components of the scattering phase matrix $R_{ij} = R_{ij}/R_{11}$.

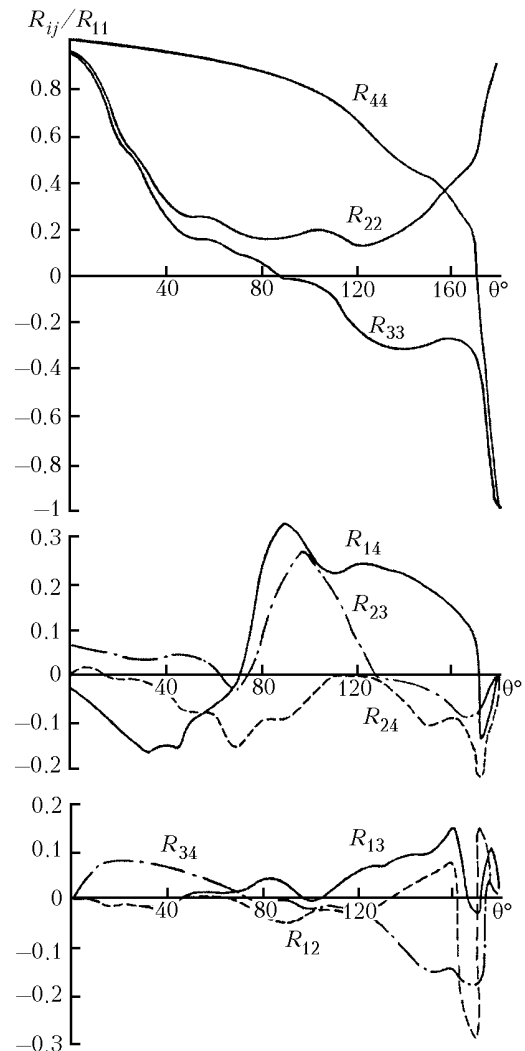


Fig. 1. Angular dependences of the scattering phase matrix components at $\alpha_s = 10^{-2}$.

The algorithm involves statistical estimation of the following integral transfer characteristics:

integrals of Stokes vector-parameters over some regions of the phase space $[X \times T]$:

$$\mathbf{I}_s = \frac{1}{c\Delta t} \int_{\Delta r^*} dr \int_{\Delta \Omega^*} d\boldsymbol{\omega} \int_{\Delta t} \mathbf{I}(\mathbf{r}, \boldsymbol{\omega}, t) dt, \quad (19)$$

where c is the speed of light, depolarization degree

$$\delta = (I_s - Q_s) / (I_s + Q_s), \quad (20)$$

orientation of the polarization plane

$$\chi = 0.5 \arctan(U_s / Q_s) \quad (21)$$

and ellipticity

$$\epsilon = \tan\left(0.5\arcsin\left[\frac{V_s^2}{(Q_s^2 + U_s^2 + V_s^2)}\right]\right). \quad (22)$$

The calculations were performed at $\phi_{\text{source}} = 0.8$ mrad, $\sigma = 0.3 \text{ m}^{-1}$, $\Delta y = 20 \text{ m}$, and $y_0 = 200 \text{ m}$ with the length of the statistical sample sufficient for maintaining the mean level of variance at the end of the sensing path within 10–15%. The solution of Eq. (1) was compared with the estimates obtained from solution of the vector and scalar equations for the equivalent medium consisting of isotropic particles with the same refractive index and the particle size distribution. For the case of weak anisotropy $\alpha_s = 10^{-4}$, the off-diagonal elements of the matrix \mathbf{R} , except for R_{12} and R_{34} , have the values smaller than 0.01, and the components of the extinction matrix χ_{14} and χ_{23} are about 10^{-3} , that is, in this case the differences between optical properties of the anisotropic and isotropic media are insignificant. Therefore, the time dependences of the intensity of single and total scattering obtained from solution of Eq. (1) almost coincide (Fig. 2) with the solution of the scalar equation. The degree of radiation depolarization (curve 3, Fig. 2) is also characterized by the same behavior, and the parameters ϵ and χ turn out close to zero.

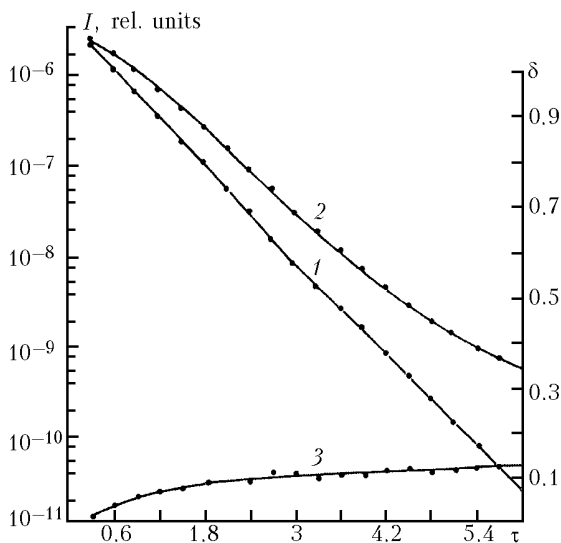


Fig. 2. Intensity of the signals due to single (curve 1) and total (curve 2) scattering and the degree of depolarization (curve 3) as functions of the optical depth at $\phi_d = 0.8$ mrad and $\alpha_s = 10^{-4}$; dots on the curves correspond to calculations for an isotropic medium.

The increase in the anisotropy factor of the medium α_s to 10^{-2} leads to an increase in the off-diagonal components of the matrix \mathbf{R} , and the components of the extinction matrix also achieve marked values $\chi_{14} = 0.0033$ and $\chi_{23} = -0.055$. It should be noted, however, that this value of α_s is extremely high for the gyrotropic medium, and the possibility of using the perturbation theory up to the first order in calculations of the scattering and extinction matrices

is still in question. For these reasons, the corresponding matrices should be considered as model ones.

In this model optical situation, the intensity of the total signal $I(\tau)$ exceeds, though only slightly, the intensity of the signal $I'(\tau)$ reflected from the medium consisting of isotropic spherical particles. This value increases with increasing $\tau = \sigma ct$ and the angular aperture of the detector ϕ_d (Fig. 3a).

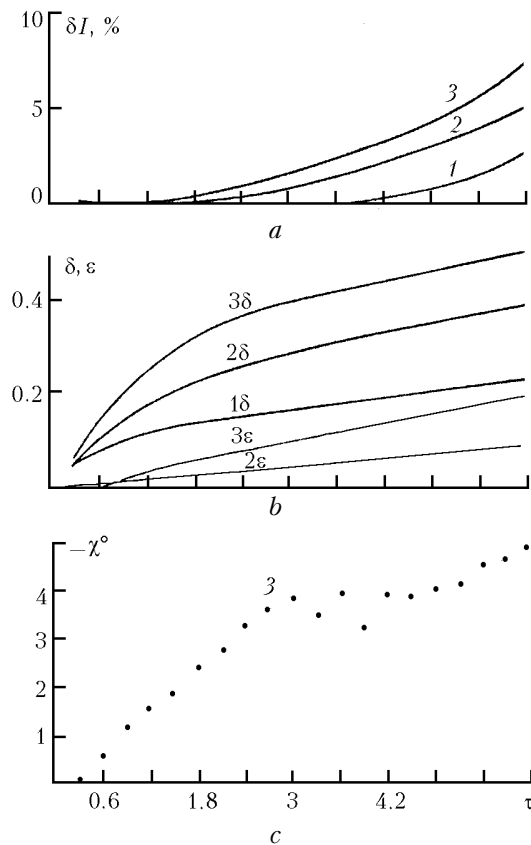


Fig. 3. Polarization properties of radiation versus dimensionless time $\tau = \sigma ct$ at $\alpha_s = 10^{-2}$. Curves 1–3 correspond to the detection angles $\phi_d = 0.8, 3,$ and 6 mrad. Indices at the digits denote the corresponding parameters.

The degree of radiation depolarization shown in Fig. 3b decreases significantly (almost twofold) as compared to the case of an isotropic medium (see Fig. 2), and at the small angles ϕ_d there are no manifestations of the anisotropy of optical properties of the medium. As the viewing angle increases, the light becomes partly elliptically polarized, and the polarization plane turns (Fig. 3c). Numerical analysis showed that the intensity of the single scattered signal $I_0 = I'$ and almost completely keeps the state of polarization (the values of $\delta, \epsilon,$ and χ are close to zero), and all the changes in the polarization structure of the echo signal are due to multiple scattering effect.

To reveal the effect of the extinction matrix on the intensity and the polarization characteristics of the echo signal, the following model problem was solved. The scattering phase matrix \mathbf{R} corresponds to

$\alpha_s = 10^{-2}$, and the components of the extinction matrix χ_{14} and χ_{23} are zero. The calculations showed that $\delta I(\tau)$ only slightly differ from those shown in Fig. 3a, and the polarization characteristics fully correspond to those shown in Figs. 3b and c. Then, keeping the matrix \mathbf{R} the same, we increased the components of the extinction matrix χ_{14} up to 0.2 and χ_{23} up to 0.055. As a result, the polarization structure transformed significantly already for the case of signal due to the single scattering. The intensity I_0 in the anisotropic medium and I'_0 in the isotropic one turn out significantly different. At the end of the path $\delta I(\tau)$ achieves $\approx 50\%$. The polarization characteristics of the single scattering signal do not keep the initial state, and the parameters δ , ε , and χ achieve marked values (Fig. 4).

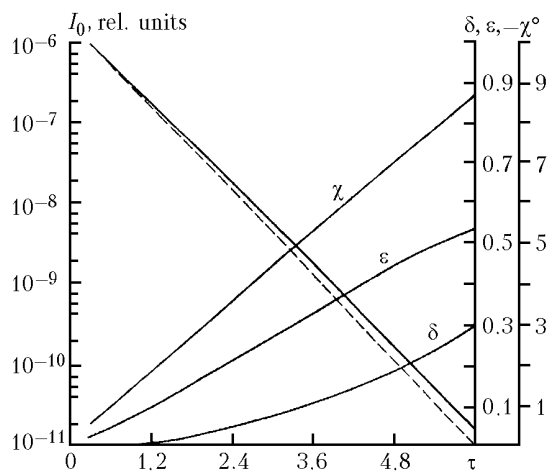


Fig. 4. Effect of the extinction matrix on the polarization characteristics of the single scattering signal: $\varphi_d = \varphi_{\text{source}} = 0.8$ mrad; dashed line is for the isotropic medium.

The angle of rotation of the polarization plane and ellipticity $I_0(\tau)$ recorded at $\varphi_d = 0.8$ mrad are almost twice as large as those for the total signal $\mathbf{I}(\tau)$ for large viewing angles ($\varphi_d = 6$ mrad), but at the smaller values of χ_{14} and χ_{23} in the matrix $\hat{\mathbf{A}}$ (see Figs. 3b and c). These features suggest that even weak medium anisotropy leads to a marked transformation of the radiation polarization structure, while the signal intensity, as in the isotropic medium, can be determined by the scalar approximation. Quite similar conclusion can also be drawn from analysis of Eqs. (18). It follows from these equations that the intensity of the single scattering echo signal (with regard for the fact that the components R_{12} , R_{13} , R_{14} are zero in the direction $\theta = \pi$) $I_0 = I'_0 \cosh_{v_{14}}$. At the

low values of the anisotropy factor, when $\chi_{14} < 10^{-2}$, $\cosh_{v_{14}} \approx 1$ up to large optical depths τ .

Conclusion

In this paper we have proposed, for the first time, an approach for constructing the algorithms for numerical solution of the nonstationary radiative transfer problem in the fully matrix form for the geometry of spatially limited beams. The results obtained show a marked manifestation of the effects of optical anisotropy of scattering particles on the polarization characteristics of lidar returns. If the abnormal increase of the anisotropy factor for aerosol particles in the atmospheric surface layer is possible, then peculiarities in the transformation of the polarization characteristics of the optical signals may be used as an extra earthquake predictor at remote polarimetric monitoring of seismic regions.

However, it should be noted that these numerical results are only tentative. In-depth investigations should be based on a more detailed study of the behavior of the optical characteristics of the medium on both the anisotropy factor and the microphysical properties of the medium.

References

1. M.B. Gokhberg, ed., *Search of Electromagnetic Earthquake Precursors* (Moscow, 1998).
2. V.I. Grigor'ev and V.S. Rostovskii, *Vestn. MGU, Ser. 3*, No. 4, 54–57 (2000).
3. A.P. Prishivalko, V.A. Babenko, and V.N. Kuz'min, *Light Scattering and Absorption by Inhomogeneous and Anisotropic Spherical Particles* (Nauka i Tekhnika, Minsk, 1984), 262 pp.
4. G.V. Rozenberg, in: *Light Propagation in Disperse Medium* (Nauka i Tekhnika, Minsk, 1982), pp. 22–36.
5. A.Z. Dolinov, Yu.N. Gnedin, and N.A. Silant'ev, *Radiation Propagation and Polarization in Space* (Nauka, Moscow, 1979), 424 pp.
6. E.P. Zege and L.I. Chaikovskaya, in: *Abstracts of Reports at II All-Union Meeting on Laser Radiation Propagation through Disperse Medium*, Obninsk (1982), Part 1, pp. 219–222.
7. S. Chandrasekhar, *Radiative Transfer* (Clarendon Press, Oxford, 1950).
8. G.I. Marchuk, ed., *Monte Carlo Method in Atmospheric Optics* (Nauka, Novosibirsk, 1976), 320 pp.
9. H.C. van de Hulst, *Light Scattering by Small Particles* (Wiley, New York, 1957).
10. V.N. Kuz'min and V.A. Babenko, *Zh. Prikl. Spektrosk.* **36**, No. 2, 305–309 (1982).
11. G.M. Krekov and R.F. Rakhimov, *Optical-Lidar Model of Continental Aerosol* (Nauka, Novosibirsk, 1982), 200 pp.